Study of different aerodynamics modifications for small axial flow fan

Anas Bin Abdul Jalil

Final Project of Mechanical Engineering Degree. Fluid Mechanics Department
Escola Politècnica Superior d'Enginyeria de Vilanova i la Geltrú (UPC)

Abstract

In this project, the effects of airfoils on the aerodynamic performance of small axial fans were investigated to improve airflow turbulence on the blade surface and generally to improve the aerodynamic performance. Two modifications were made on the blades surface to know why and how the modifications affect the aerodynamic performance. The 3D steady numerical simulation for all models done by using CFD commercial software NX Siemens PLM version 10. The N-S equations with finite element analysis and the standard k-ε turbulence model were adopted to carry out the steady simulation calculation. A comparison between experimental results and numerical simulation also have been carried out to see how the modifications affect the aerodynamic performance and static characteristics of the fan. The effect of the winglet and shark-fin blade designs were analysed. It is concluded that the method of adding winglet to the prototype blade has an influence on reducing vorticity at the tip of the blade. The results show that by adding shark fin blade on the suction surface of the blade can channel the turbulence and at the trailing edge of the blade.

1. Introduction

A small axial fan is widely adopted in electronic field. Mainly it is used in a personal computer because of their reliable and simple structures. The cooling fans force the air to flow and at the same time it generates aerodynamic noise. The flow is driven by centrifugal force that cause by fan rotation.The flow field between the stationary casing and the rotor tip of small axial fan is complex because of the annulus wall boundary layer, the rotor wake and the leakage flow. Shape of blades profile also play an important role in the performance of the fans and their efficiency.

Pressure difference across the blade width generates air flowing through the gap at the blade tip. The tip of the blade has the highest circumferential velocity. The air-gap width and its shape significantly affect integral aerodynamic characteristic and acoustic emission of fan. Problem of the air-gap leakage and generation of the induced swirling have been frequently discussed by different authors.Passive control technique by modifying end-plate according to the concept of the leakage-vortex rotation number improved the efficiency with increase peak performance [1]. By adding tip end-plate which have geometry of 2 mm width inconstant length of chordwise has decrease vorticity variation on the surface blades. It helps to reduce broadband noise in the far field but not in reducing discrete noise in the near field [2].

Zhang et al [3] studied the effect of the irregular airfoils on the aerodynamics performance of small axial flow fan. Two irregular designs were applied to the normal airfoil. One of them have several convex grooves are bound in blade pressure surface and the other one has a wave-shaped edge which is bound to the blade trailing edge of the fans. The result shows the total pressure of the three airfoils are relatively similar. The performance curve of airfoil that have several convex grooves has a smooth feature. It also changes the turbulent structure near the wall and compress the sphere influence of the vortex while the wave-shaped edge airfoil changes the flow direction of vortex shedding. Zhang et al [4] present that tip flange of the fan has a certain influence on the characteristics of fan. It contributes to forming tip vortex shedding. The investigation used the numerical simulation and experimental methods to investigate the effect of tip flange on tip leakage flow.

The influence of saw tooth trailing edge serration has been investigated using stereoscopic particle image velocimetry (PIV). It shows that flow will undergoes important changes in various mean flow and turbulence statistic measures [5]. Zhu et al [6] studied aerodynamic performance of small axial flow fan with splitter blade. Static characteristics of small axial fan flow can be improved with splitter blades. Generally, the static pressure rise of axial flow fan with splitter blade is higher than an axial flow fan without splitter blade but the efficiency is closely similar between them.

In this paper, 2 modifications were applied to the airfoils of the fans. Numerical simulation and experiments were performed to analyse the static characteristic and internal flow feature of the small axial fan.

2. Study of the fans

A small axial flow fan, LYF DC 12V 4PIN 8cm 8015s brushless was selected as the sample fan in this paper. The rotor has 7 rotor blades. The diameter of the impeller of the impeller is 76 mm, the hub diameter is 34.5 mm, hub to tip ratio 0.45, tip clearance 1 mm, a rated rotating speed of 2000 r/m and rated air flow is 45 CMF.

Based on the prototype (model 1), 2 modified models were applied which are the geometry of the modification that can be made is 2 mm width which is in-constant along the chordwise or called as winglet (model 2) and a geometry of

shark fin blade (model 3). The spacing between the 3-shark fin blade on the surface of blade is 5 mm. Figure 1 shows the geometry of model 1, 2 and 3.

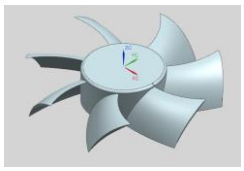

(a) *Model 1*

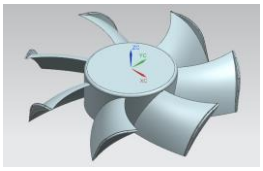

(b) *Model 2*

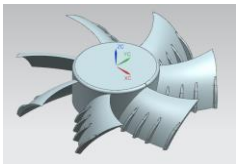

(c) *Model 3*

Fig. 1. *Geometry of different model.*

3. Numerical procedure

A. Computational domain

The computational domain for the simulation consists of the rotating fluid area, the inlet and outlet ducts. For the simulation purposes, the length of the inlet duct is 40mm and the diameter is 200mm while for the outlet duct is 400mm length and the diameter is 200mm as shown in Fig. 2. The fan hub was set as the coordinate origin.

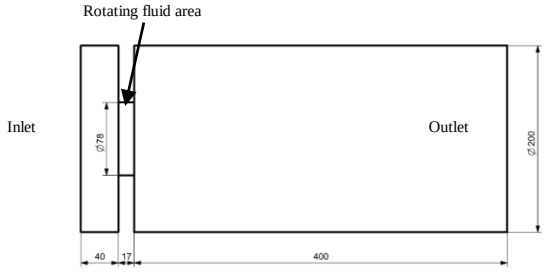

Fig. 2. *Computational domain.*

B. Mesh

The NX software was used to generate the grid for the computational domain. 4-noded tetrahedral element (TET4) was used to mesh all the element in the rotating fluid area and in the regions of the inlet and outlet ducts as shown in Fig. 3.

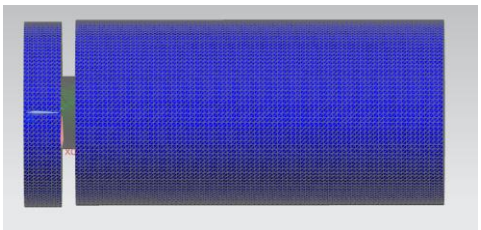

Fig. 3. *Mesh.*

Large size of elements was used in flow simulation, as shown in Fig. 4. to verify if the solution is element size independent or not. An element counts larger than 41000 does not produce a visible different in average velocity of rotating fluid area.

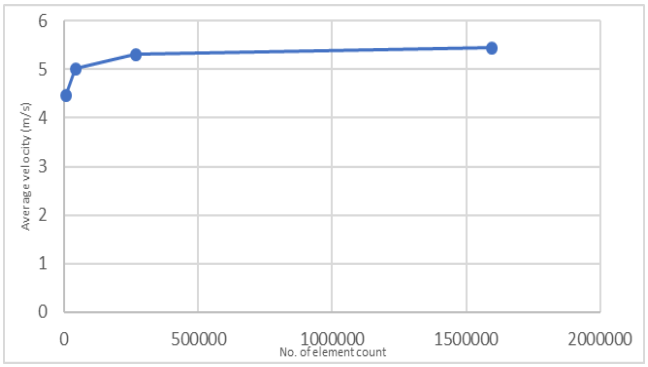

Fig. 4. *Grid sensitivity test result.*

C. Boundary conditions

Flow boundary condition for inlet duct is set as an opening and outlet duct have outlet mass flow which is $\dot{m}$=0.0242 kg/s. It external condition is ambient, external pressure type is absolute and external absolute pressure is ambient. Mixing plane simulation object was used to interface fluid regions between inlet duct, rotating fluid area and outlet duct. For the rotating fluid area, moving frame of reference simulation object was used to model the effect of rotating fan on the surrounding fluid. The rotation velocity used was 2000 rpm. The solid wall such as vane surface and hub satisfy the no-slip condition in the computational domain.

D. Governing equations

The calculations were performed with a commercial software NX Siemens PLM version 10. The basic equations that are used for the numerical simulations are continuity equation and Navier-Stoke equation. In Cartesian coordinates, continuity equation is:

$$\nabla \cdot \vec{V} = 0 \tag{1}$$

Where $\vec{V}$ velocity vector of the air flow. Navier-Stoke equation is described by

$$\rho g_i + F_i - \nabla p + \nabla \cdot \tau_{ij} = \rho \frac{D\vec{v}}{Dt} \tag{2}$$

where ρ is the density fluid, P is a pressure, g_i is gravity, τ_{ij} is the Reynolds stress component and F_i is external body force.

E. Solving method

The Mach number at the tip of blade is 0.02M, which is inferior to the limit of incompressible fluid (0.3M). RANS k-ε turbulence model was used to solve the steady simulation. For the simulation in this project, all the residuals reach at least 10^{-4}.

4. Comparison of the experimental and numerical results of the axial fan

To measure axial fan rotational speed, a Lutron digital tachometer (DT-2236) was used. The voltage was set at 12 V and the current was 0.18 A by using Power Supply FAC-662B PROMAX. The measurements were repeated on several occasion and axial fan was maintain to rotate for 1

minute before the measurement was taken. The axial fan speed was n = 2000 rpm.

To validate the simulations, a comparison has been made between the experimental and numerical results. Average velocity at several points have been taken experimentally by using the anemometer GVA0430 with an accuracy ±2%. Inlet speed and outlet speed at various points based on Fig. 5. were measured using an anemometer.

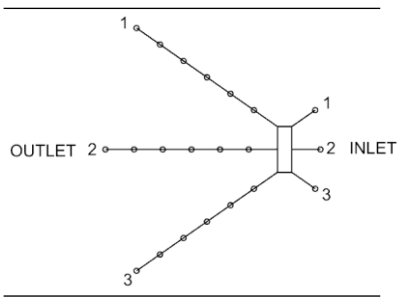

Fig. 5. *Points where the anemometer was placed during the measurement*

For the numerical results, average velocity at 5 cm and 30 cm from the axial fan were measured. For 5 cm, average velocity is 2.79 m/s for numerical simulation and the experimental value was 2.8 m/s. At 30 cm, the numerical velocity is 0.814 m/s. The value is not very far from the experimental value which is 0.96 m/s. Fig. 6 shows the graph of comparison between experimental results and numerical solution.

Simulation values obtained were inferior to the experimental values showing the great variation within a distance of 15 cm and the error decreasing towards the ends of flow field. There are always exists a discrepancy between experimental measurements and numerical simulation for any engineering problems. It may be due to either simulation error or experimental error or both.

From the results obtained, it can be concluded that the numerical calculation methods are feasible and reliable for this project.

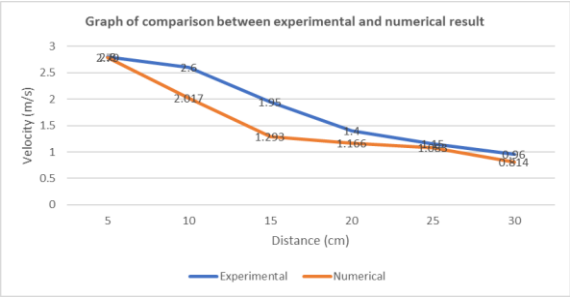

Fig. 6. *Graph of comparison between experimental and numerical results.*

5. Mechanism analysis of the modified models

The internal flow characteristics of a cooling fan are the key factors that affect the static characteristics and aerodynamic performance. Therefore, by analysing the internal flow characteristics of a fan is a feasible method to determine the mechanism of their regular designs. Analysing can be done by observing axial velocity contour of the meridional plane the fans.

Fig. 7. shows the axial velocity contours of the meridional plane (X=0) of the airfoils when the rotational velocity is 2000 rpm and the mass flow rate is 0.0242 kg/s. Generally, vortexes were formed at the downstream of the hub at all models and at model 3, the vortexes formed at a middle of the downstream were slightly smaller than in the other models.

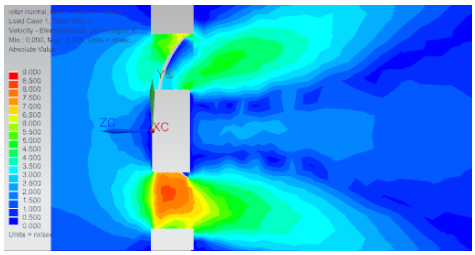

(a) *Model 1*

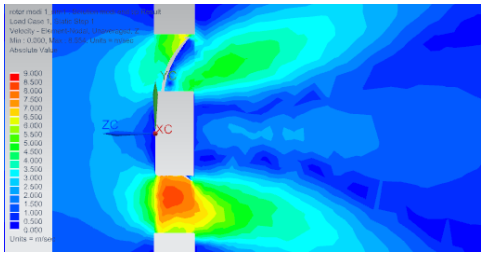

(b) *Model 2*

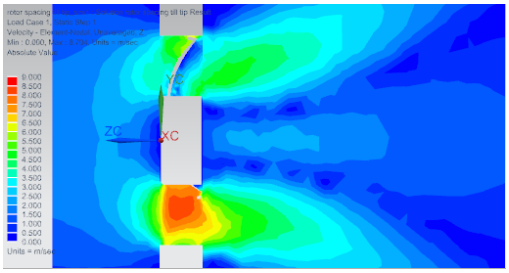

(c) *Model 3*

Fig. 7. *Axial velocity contours of the meridional plane (X=0).*

As we can see, Fig. 8, at the tip of blade for model 1, its velocity is higher compare to velocity at the tip for model 2 and 3. Winglet at model 2 and model 3 change the rate of velocity at the tip of blade. It can be seen that vortex mainly occurs at the hub of model 2 and 3. At model 3, the vortexes were scatter into smaller vortexes. The shark fin blade at the suction side caused more channel turbulence [7]. At model 2, the vortex formed at hub much bigger than at model 3.

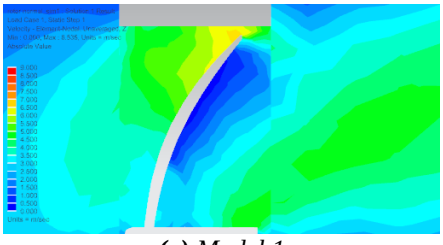

(a) *Model 1*

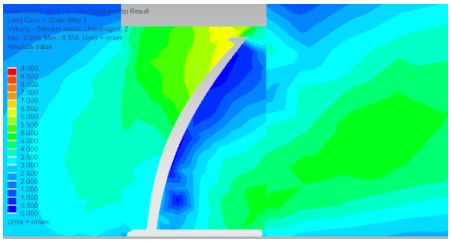

***(b)** Model 2*

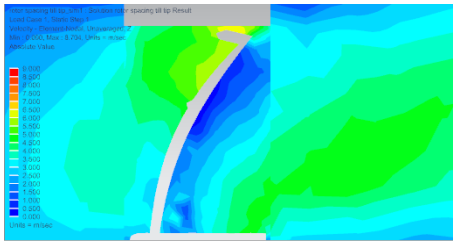

***(c)** Model 3*

***Fig. 8.** Detail of axial velocity contours of the meridional plane (X=0).*

Fig. 9. shows the static pressure contours of the meridional plane for model 1 and model 2. The difference of static pressure between suction surface and pressure surface is shown in the figure by 2 points. The difference of 2 points at model 2 (9.726 Pa) is smaller than model 1 (11.766 Pa), therefore vorticity at the tip of model 2 is smaller [8].

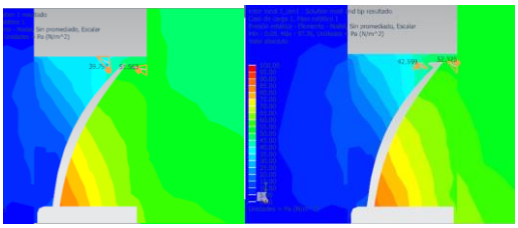

***(a)** Model 1* ***(b)** Model 2*

***Fig. 9.** Static pressure contours of the meridional plane (X=0) of the fans.*

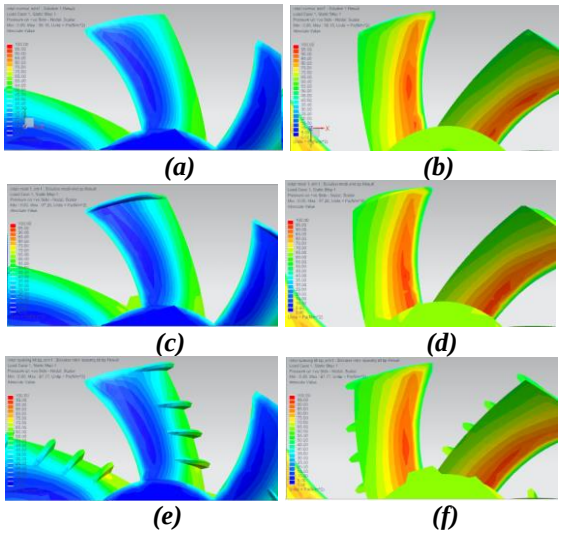

(a) ***(b)*** ***(c)*** ***(d)*** ***(e)*** ***(f)***

***Fig. 10.** Static pressure contours distribution of the blade suction surface and the pressure surface of the three models: (a) Suction surface of model 1; (b) Pressure surface of model 1; (c) Suction surface of model 2; (d) Pressure surface of model 2; (e) Suction surface of model 3; (f) Pressure surface of model 3.*

Fig. 10. shows the contour distribution of static pressure on suction surface and pressure surface for three models of axial fan when the mass flow rate is 0.0242 kg/s. It can be seen that the static pressure of pressure surface is generally higher than that of suction surface. The pressure gradient between the suction surface and the pressure surface is the key factor that cause leakage around the tip or known as a tip leakage vortex.

Adverse pressure gradient occurred at the suction surface because the airflow passes through side which have less pressure to the side that have higher pressure. This can cause boundary layer separation that will form vortex (wake). At the pressure surface of the blade, the gradient pressure is favourable to the flow because the airflow passes through higher pressure to less pressure. Therefore, flow separation does not occur.

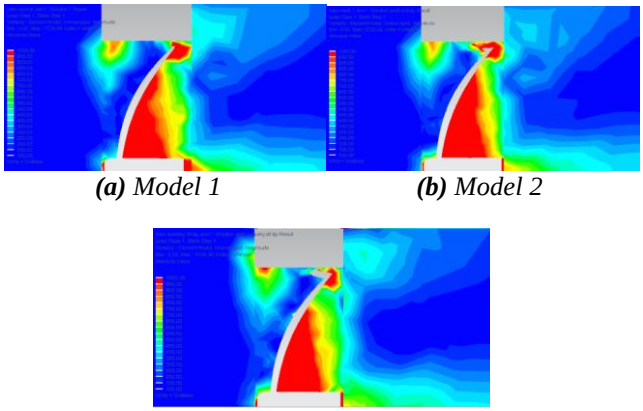

***(a)** Model 1* ***(b)** Model 2*

***(c)** Model 3*

***Fig. 11.** Vorticity contours distributions of the meridional plane (X=0) of the fans.*

Several vortex formations can be seen clearly at Fig. 11. At model 3, the vortex keeps changing at the suction surface. The shark fin blade caused the smaller vortex occurs at the pressure surface. It advantage is to increase the airflow [7].

At the tip of blade of model 1 and 3, the vortex formed at tip of the pressure side of blade while for model 2, the vortex formed around the tip of blade. At the downstream, the big vortex was scatter to smaller vortexes at model 2 while at model 3 the vortex was slightly bigger than at model 1. The vortex that form near the hub for model 3 is little bit smaller than the other models.

In order to further study the internal flow characteristics about fan, velocity distribution was analysed. Fluid flow was observed from three different axial cross-sections, which are cross-sectional Z = -2 mm (inlet of passage), Z = -7,5 mm (intermediate of passage), Z = -13mm (outlet of passage) (Figure 12).

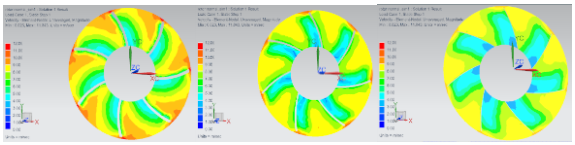

(a) (b) (c)

Model 1

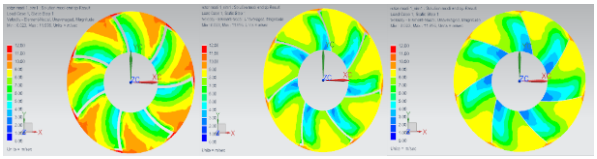

(a) (b) (c)

Model 2

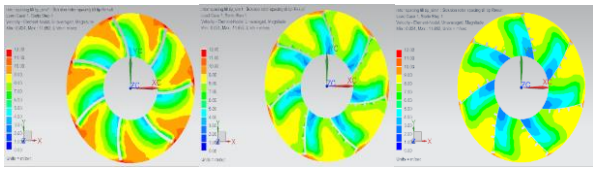

(a) (b) (c)

Model 3

Fig. 12. *Three different axial cross-sections, which are cross-sectional a:(inlet of passage), b: (intermediate of passage), c: (outlet of passage).*

Fig. 12. shows the speed of airflow when it enter the rotating body. Generally, speed of airfow is the highest at the tip of blade. Airflow is very fast when it enter the passage then it velocity decrease gradually until it pass through the outlet passage. The airflow at the outlet of passage is more stable where the velocity is mainly between 9 m/s to 4 m/s.

The differences of velocity at different passage can be caused by the diffuser effect, by increasing the passage section through the blades [9]. Diffuser effect can reduce average velocity of flow and increase it average pressure. This will lead to boundary layer separation due to adverse pressure gradient.

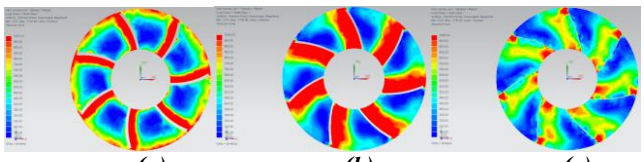

(a) (b) (c)

Model 1

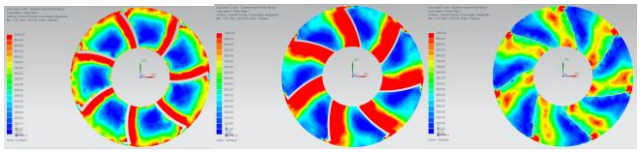

(a) (b) (c)

Model 2

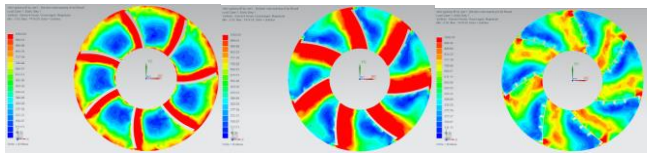

(a) (b) (c)

Model 3

Fig. 13. *Three different cross-sections of vorticity, which are cross-sectional a:(inlet of passage), b: (intermediate of passage), c: (outlet of passage).*

Fig. 13 shows the vorticity in three sections of different models. It can be observed that the vorticity at model 3 is generally smaller than the other models.

The formation of vortexes for model 1, Fig. 13(c), occurred clearly at tip of blade and near the hub. For model 2, the vortexes at the outlet passage occurred mostly near to the winglet and at the hub, but the vortexes are located in a larger area of the passage. It can be seen clearly that at model 3(c) the vortex occurs in the space between the suction surface and the pressure surface along the way from hub to the winglet. Near the hub, vortex intensity at model 1 is slightly bigger than the other models.

6. Conclusion

The project introduced 2 modifications on small axial fan which are winglet (model 2) and shark fin blades (model 3). With the help of numerical simulation and experimental testing, the effect of modifications that have been made on the aerodynamic performance, static pressure characteristic and the internal flow field were determined. The mechanism analysis of the modified models was discussed. The conclusions are summarized as follows:

1) The difference between the models 1 and 2 shown that the presence of a winglet reduces the vortices created by the reduction of differential pressure between the pressure surface and suction surface at the tip of blade.

2) Diffuser effect can reduce average velocity of flow and increase it average pressure. This will lead to boundary layer separation due to adverse pressure gradient.

3) Vortexes formed at downstream at model 2 were much smaller than the other models. In model 3, the vorticity near the hub was smaller than the other models.

4) Vortexes were more concentrated at the tip of blade and near hub for model 1 but it was different for model 2 and 3. The vortexes occurred along the blade between the passage from hub to tip of blade.

5) Adding shark fin blade at the suction surface of blade can help to channel the turbulence therefore reduce the vortex effect near the hub and at trailing edge of blade.

The decreasing vorticity that have been observed in the flow of model 2 and model 3 can be relate with a possibility of noise reduction for axial fan as have been told by the manufacturer [7] and the authors [2],[8].

References

[1] A. Corsini, A. G. Sheard, “Tip End-Plate Concept Based on Leakage Vortex Rotation Number Control,” Journal of Computational and Applied Mechanics, Vol 8., No. 1, pp.21-37, 2007.

[2] H. Mao, Y. Wang, P. Lin, Y. Jin, S. Tosh, and K. D. Heuy, “Influence of Tip End-plate on Noise of Small Axial Fan,” *J. Therm. Sci.*, vol. 26, no. 1, pp. 30–37, 2017.

[3] L. Zhang, Y. Jin, and Y. Jin, “An investigation on the effects of irregular airfoils on the aerodynamic performance of small axial flow fans,” *J. Mech. Sci. Technol.*, vol. 27, no. 6, pp. 1677–1685, 2013.

[4] L. Zhang, Y. Jin, and Y. Jin, “Effect of tip flange on tip leakage flow of small axial flow fans,” *J. Therm. Sci.*, vol. 23, no. 1, pp. 45–52, 2014.

[5] C. Arce León, D. Ragni, S. Pröbsting, F. Scarano, and J. Madsen, “Flow topology and acoustic emissions of trailing edge serrations at incidence,” *Exp. Fluids*, vol. 57, no. 5, p. 91, 2016.

[6] L. Zhu, Y. Jin, Y. Li, Y. Jin, Y. Wang, and L. Zhang, “Numerical and experimental study on aerodynamic performance of small axial flow fan with splitter blades,” *J. Therm. Sci.*, vol. 22, no. 4, pp. 333–339, 2013.

[7] ZM-SF2 Shark’s Fin Blade 92mm Silent Fan. [Online]. Available:http://www.zalman.com/contents/products/view.html?no=351

[8] S. A. Beskales, Samir S. Ayad, M. G. Higazy and O. E. Abdellatif, “The Effect of Tip End-blade Geometry on the Axial Fans Performance,” presented at Eleventh International Conference of Fluid Dynamics, Alexandria, Egypt, 2013.

[9] "Máquinas Axiales," Maquinas Para Fluidos 1, Instituto de Mecánica de Los Fluidos e Ingeniería Ambiental. [Online]. Available:https://www.fing.edu.uy/imfia/cursos/maq_flu_1/teorico/7-Axiales.2009.pdf